Primljen / Received: 24.9.2025.
Ispravljen / Corrected: 23.5.2026.
Prihvaćen / Accepted: 22.6.2026.
Dostupno online / Available online: 10.8.2026.

# Experimental investigation of eccentric strip footing near existing foundation in sand

Authors:

Prof. **Abdelmadjid Abdi**, PhD. CE
Echahid Cheikh Larbi Tebesi University, Algeria
Faculty of Science and Technology
Department of Civil Engineering
abdelmadjid.abdi@univ-tebessa.dz
**Corresponding author**

Prof. **Rafik Boufarh**, PhD. CE
Echahid Cheikh Larbi Tebessa University, Algeria
Faculty of Science and Technology
Department of Civil Engineering
Laboratory of Applied Civil Engineering (LGCA)
rafik.boufarh@univ-tebessa.dz

Prof. **Hsaine Chabbi**, PhD. CE
Badji Mokhtar University Annaba, Algeria
Faculty of Technology
Department of Civil Engineering
Laboratory of Soils and Hydraulics
hsain.chabbi@univ-annaba.dz

Research Paper

Abdelmadjid Abdi, Rafik Boufarh, Hsaine Chabbi

## Experimental investigation of eccentric strip footing near existing foundation in sand

This paper reports on an experimental study of the effect of an existing foundation on the behaviour of a newly constructed strip footing subjected to eccentric loading in sand. Model tests were conducted in a laboratory tank using dry uniform sand prepared by pluviation. The new footing was tested under centric and eccentric loadings at different eccentricity ratios (e/B) and spacing ratios (x/B) relative to the existing footing. The load–settlement response, ultimate bearing capacity, and influence of the eccentricity direction were evaluated. The results indicate that the bearing capacity decreases with increasing eccentricity and spacing, whereas the soil-structure interaction becomes negligible at $x/B \geq 3$, wherein the footing behaves independently. The bearing capacity was consistently higher when the eccentricity was directed towards the existing footing. An eccentric interaction factor ($E\zeta$) was introduced, with a maximum value of 1.40 at $x/B = 0.5$ for small e/B. Two failure modes were identified, providing valuable insight into the design of closely spaced strip footings under eccentric loading.

**Key words:**
**strip footing, eccentric, existing, experimental, spacing, interference**

Prethodno priopćenje

Abdelmadjid Abdi, Rafik Boufarh, Hsaine Chabbi

## Eksperimentalno istraživanje ekscentrično opterećenog trakastog temelja u blizini postojećeg temelja u pijesku

U radu su prikazani rezultati eksperimentalnog istraživanja utjecaja postojećeg temelja na ponašanje novoizgrađenog trakastog temelja podvrgnutog ekscentričnom opterećenju u pijesku. Modelska ispitivanja provedena su u laboratorijskom spremniku, koristeći suhi jednoliki pijesak pripremljen metodom pluvijacije. Novi temelj ispitan je pri centričnom i ekscentričnom opterećenju za različite omjere ekscentričnosti (e/B) i razmake između temelja izražene omjerom (x/B) u odnosu na postojeći temelj. Analizirani su odnos opterećenja i slijeganja, nosivost te utjecaj smjera ekscentričnosti. Rezultati pokazuju da se nosivost smanjuje s porastom ekscentričnosti i razmaka između temelja, a međudjelovanje tla i konstrukcije postaje zanemarivo pri $x/B \geq 3$ kada se temelj ponaša neovisno o susjednom temelju. Nosivost je dosljedno bila veća kada je ekscentričnost bila usmjerena prema postojećem temelju. Uveden je faktor međudjelovanja uslijed ekscentričnosti ($E\zeta$), čija je najveća vrijednost iznosila 1,40 pri $x/B = 0{,}5$ za male vrijednosti omjera e/B. Utvrđena su dva karakteristična mehanizma sloma, što pruža vrijedne spoznaje za projektiranje gusto raspoređenih trakastih temelja pod ekscentričnim opterećenjem.

**Ključne riječi:**
**trakasti temelj, ekscentričnost, postojeći temelj, eksperimentalno istraživanje, razmak, međudjelovanje**

## 1. Introduction

The rapid urbanisation of metropolitan areas worldwide has intensified the demand for efficient land use, and necessitated constructing new structures near existing buildings [1, 2]. In densely populated urban centres wherein buildable land is scarce, geotechnical engineers routinely encounter situations in which the foundations of a planned structure must be designed within the zone of influence of pre-existing foundations. This spatial overlap generates complex soil–structure interactions that can significantly affect the load-bearing capacity, settlement response, and failure mechanism of the newly constructed foundation, creating a multifaceted challenge that conventional design methods are ill-equipped to handle [2–4].
The classical bearing capacity theory, as developed by Terzaghi [5], extended by Meyerhof [6], and further generalised by DE Beer [7], is based on three idealising assumptions: foundation isolation, symmetric stress distribution about the load axis, and a homogeneous half-space. Within this framework, eccentric loading is accommodated through the effective-width concept, whereby the eccentricity $e$ reduces the nominal footing width $B$ to an effective dimension $B' = B - 2e$, and the ultimate bearing capacity is computed for this reduced width under a centrically applied load [6]. Controlled laboratory investigations by Prakash and Saran [8], Sadoglu et al. [9], and Das and Maheshwari [10] have confirmed that the bearing capacity of an isolated strip footing decreases monotonically with an increasing eccentricity ratio ($e/B$) owing to the progressive reduction in the effective contact area and the growing moment demand transferred to the supporting soil. Although these solutions are well established and codified in international design standards, they fundamentally assume a symmetric, undisturbed stress field, which is violated when a loaded foundation is adjacent.
The interactions between closely spaced strip footings have been investigated since Stuart [11] first demonstrated that two simultaneously loaded footings on dense sand can exceed the bearing capacity of an equivalent isolated footing when the clear spacing falls below a critical threshold. This beneficial interference is conventionally quantified by the interference factor $\zeta$, defined as the ratio of the ultimate bearing capacity of a footing in the presence of an adjacent foundation to that of an equivalent isolated footing under centric loading, with values of $\zeta > 1$ and $\zeta < 1$ indicating beneficial and detrimental interference, respectively. The physical mechanism underpinning this beneficial interference is the mutual confinement of the overlapping passive Rankine zones beneath the adjacent footings, which suppresses the lateral soil displacement, deepens the failure surface, and elevates the mobilised friction angle in dense, dilatant sands [12, 13]. Kumar and Bhoi [14] have confirmed this mechanism experimentally and reported a peak capacity at a critical clear-spacing ratio, beyond which $\zeta$ declines towards unity. Mabrouki et al. [15] have reproduced this behaviour numerically using finite element analysis and found that the greatest enhancement for rough-based footings occurs at a spacing ratio ($x/B$) between 0.1 and 0.5. Gupta and Sitharam [16] have reported a maximum interference factor of $\zeta \approx 1.25$ in dense sand for two interfering square footings, while Ghosh and Kumar [17] have demonstrated that the beneficial interaction persists across a range of layered cohesionless profiles. Detrimental interference has also been previously reported. Ghazavi and Dehkordi [18] have showed that capacity reductions occur when the clear-spacing ratio falls below a secondary critical threshold smaller than that associated with the peak capacity, generating a non-monotonic response that transitions from enhancement at moderate proximity to degradation at very close spacing. Ekbote and Nainegali [19] have attributed this degradation to the premature coalescence of the failure surfaces within the soil wedge confined between the two footings, which precludes the development of the Prandtl mechanism and forces a failure along a kinematically weaker path. The apparent contradiction between the beneficial and detrimental findings can be resolved by recognising that the interference response is governed by the interplay of the soil relative density, interfooting spacing, soil friction angle, and load level carried by the existing footing [2, 11, 15]. In dense, dilatant sands, the strain hardening and volumetric expansion in the passive zone favour beneficial interactions, whereas in loose sands, the volumetric collapse and early shear-zone coalescence promote the detrimental behaviour. Kouzer and Kumar [20] have demonstrated that for existing-footing load levels exceeding approximately 50 % of the failure load (0.5*Qu), detrimental effects can emerge even at friction angles that would otherwise favour beneficial interference.
A configuration of practical significance, termed the new-footing-near-existing-footing problem, arises when a new footing is constructed adjacent to an existing foundation that has already sustained a known working load. This scenario is inherently asymmetric: the pre-existing stress field set by the loaded foundation fundamentally alters the soil state before the new footing is constructed, such that the interaction cannot be modelled as a symmetric, simultaneously loaded problem. Kouzer and Kumar [20] have studied this configuration numerically for equal-width strip footings in medium-dense sand and identified a strongly nonmonotonic capacity response at higher friction angles that is sensitive to the existing-footing load level. Nainegali et al. [21] have investigated the interaction between a proposed footing and an existing footing resting on nonlinearly elastic cohesionless soil using finite element analysis. Their results demonstrated that the interference effect significantly alters both the bearing capacity and settlement response, with the magnitude of the interaction depending on the spacing ratio and soil density. They identified the optimum spacing at which the interference effect is maximum, and found the response to be asymmetric when the existing footing is preloaded. Moreover, the study showed that dense soils are more sensitive in terms of bearing capacity, whereas loose soils exhibit greater settlement variations, emphasising the combined influence of the soil state and loading sequence on the footing interaction. Schmüdderich et al. [22] have employed finite-element limit analysis to map the combined influence of the footing-size ratio, spacing, friction

angle, and existing load level, establishing that the capacity of the new footing reaches a maximum at a spacing ratio whose value depends on both the friction angle and load state of the existing foundation. These studies have confirmed that the new-footing-near-existing-footing problem constitutes a distinct class of soil–structure interactions that require dedicated experimental and analytical treatment.

Despite this body of numerical research, a critical experimental gap remains, as no previous study has systematically investigated the combined effect of load eccentricity and the presence of a preexisting loaded foundation on the bearing capacity and failure mechanism of a new strip footing. This gap has direct practical consequences, as eccentric loading is routine in foundation engineering, arising from wind and seismic action, differential column reactions, crane–girder forces, and construction tolerances, and is frequently applied to footings located adjacent to preexisting structures. When the eccentricity is superimposed on the already asymmetric stress field generated by a loaded neighbouring foundation, the load-transfer mechanism and failure kinematics cannot be reliably predicted by combining the effective-width reduction with the interference factor $\zeta$. The direction of the eccentricity relative to the existing footing introduces a geometrically controlled asymmetry: the eccentricity directed towards the neighbouring foundation amplifies the stress concentrated in the confined soil wedge, whereas the eccentricity directed away from it shifts the failure surface to the distal side, producing qualitatively different reductions in both the capacity and failure mode. Current design standards, including Eurocode 7 [23] and related guidance [24], do not provide for this combined scenario, leaving practitioners without a rational basis for design and creating the potential for unconservative outcomes. Therefore, experimental data are urgently required to characterise this problem quantitatively and furnish a validated dataset for future numerical and analytical modelling.

This study aimed to investigate the behaviour of a strip footing constructed adjacent to a pre-existing loaded footing experimentally under eccentric loading conditions in dry sand. Unlike previous studies that have predominantly examined the footing interference after concentrically or eccentrically loading the isolated footings, the combined impact of the load eccentricity and footing interaction has not been explored experimentally. Accordingly, the main contribution of our study lies in supplying a comprehensive experimental dataset that captures the coupled influence of the spacing ratio, eccentricity magnitude and direction, and existing footing load level on the bearing capacity, load–settlement response, and failure mechanisms. In addition, this study systematically evaluates the influence of the spacing ratio, eccentricity magnitude, and eccentricity direction on the bearing capacity, load–settlement behaviour, and failure mechanism of closely spaced strip footings, and introduces the eccentric interaction factor ($E\zeta$) as a unified dimensionless parameter to quantify the combined effects of the geometric interaction and load eccentricity.

## 2. Problem statement

The behaviour of the isolated strip footing under eccentric loading has been the subject of several research works [6, 8, 25, 26]. The failure load and stress distribution beneath the strip footing are symmetric with respect to the footing axis, regardless of whether the load eccentricity is directed to the left or right (Figure 1). However, this symmetric distribution is lost when adjacent to an existing footing because the interaction between the two foundations alters the stress-transfer mechanism (Figure 2). Two distinct cases were considered in this study stemming from such loss of symmetry wherein the load eccentricity is directed towards and away from the existing footing, respectively.

In the following sections, the eccentricity values are considered positive and negative when oriented towards and away from the existing footing (Figures 2.a and 2.b).

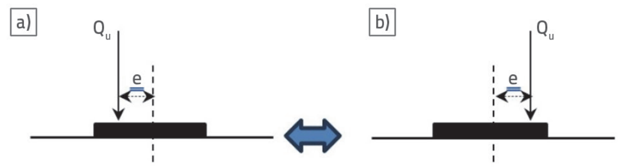


**Figure 1. Isolated footing subjected to eccentric loading: a) load shifted to the left of the footing axis; b) load shifted to the right**

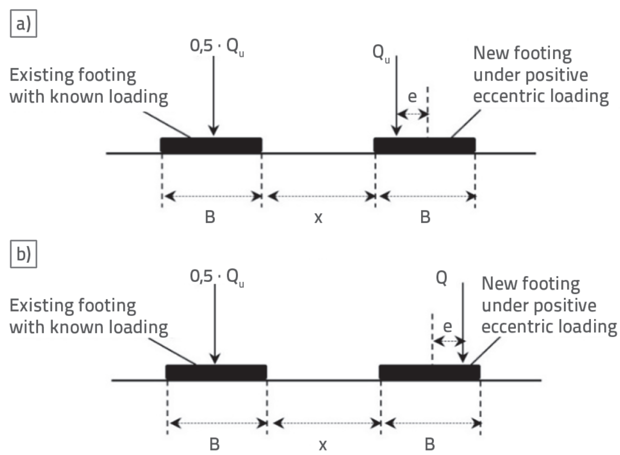


**Figure 2. New footing subjected to eccentric loading adjacent to an existing footing: a) positive eccentricity (towards the existing footing); b) negative eccentricity (away from the existing footing)**

## 3. Experimental modelling

### 3.1. Test equipment

In this study, the model tests were conducted in a rigid steel tank with internal dimensions of 1.50 × 0.50 m (plan) and 0.60 m (depth). One side of the tank was constructed with 10 mm thick Plexiglas to control the placement and compaction of the soil layer and observe the footing failure mechanisms. The

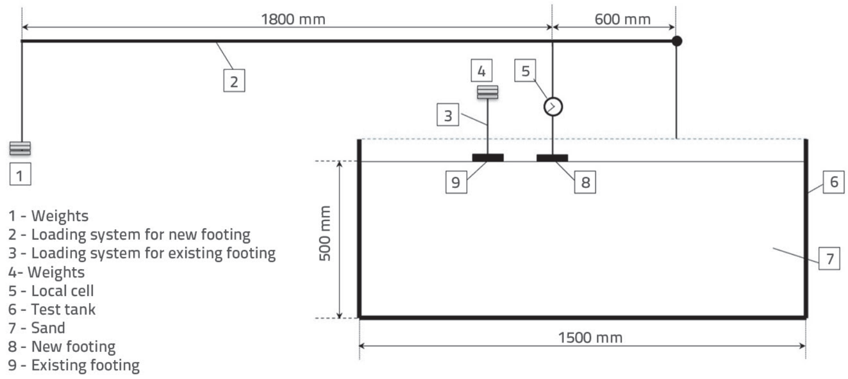


**Figure 3. Schematic of the model test tank and loading apparatus**

two footing ends were smoothed to minimise their frictional interactions with the inner sides of the tank and reduce the boundary effects.


**Figure 4. Sequence of the loading applied to the two footings: a) load application on the existing footing; b) loading the new footing 1 h after loading the existing footing**

The model footings were constructed from rigid steel with a width of 100 mm and length of 498 mm. In all tests, both the footings were placed directly on the prepared soil surface. Sandpaper was affixed to the undersides of both footings to simulate rough contact conditions and prevent slippage.

The loading system consisted of two separate components, with the first designed to apply a direct load to the existing footing. The second one comprised a rigid steel beam of length 2.4 m , which was used to apply the loads to the new strip footing in increments of 10 kg (Figures 3 and 4). The applied load was recorded at the point of application using a load cell with a capacity of 15 kN. The settlement of the new footing was measured using a mechanical dial gauge with a range of 10 cm positioned at the point of load application.

### 3.2. Soil used in the model tests

The soil used in the model tests was a medium sand collected from the Tebessa region in northeastern Algeria. This soil was oven-dried before testing and sieved to remove the oversized particles and impurities. It was classified using a standard grain size distribution analysis (Figure 5) as SW, i.e., well-graded sand, according to the unified soil classification system (USCS) [27]. The sand exhibited negligible plasticity, ensuring that its mechanical response was dominated by the frictional behaviour. This material was selected for its uniformity and ease of preparation, making it well suited for controlled laboratory model tests. The sand was deposited in the test tank through pluviation from a constant height and compacted in successive lifts of 5 cm thickness until the target height of 50 cm was achieved, ensuring a uniform density throughout the soil bed. The unit weight of the sand, determined in accordance with ASTM [27] standards, was approximately 16.36 kN/m$^3$, which is typical for quartz-based sands. The friction angle corresponding to this unit weight was determined to be 37° via direct shear testing. The main properties of this sand are summarised in Table 1.

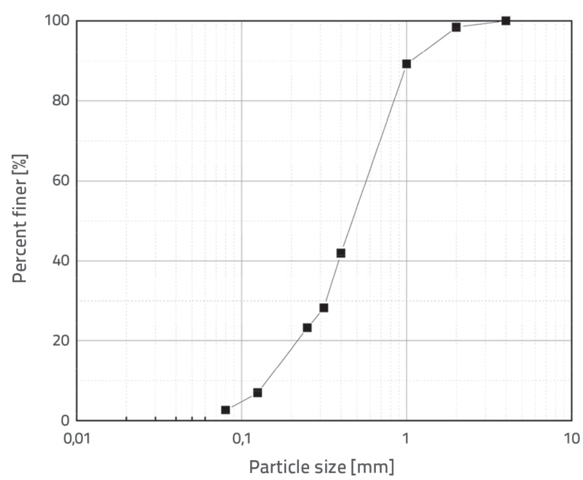


**Figure 5. Grain size distribution curve of the sand employed in the model tests**

**Table 1. Soil parameters**

| Properties | Value |
|---|---|
| Coefficient of uniformity, $C_u$ | 3.73 |
| Coefficient of curvature, Cc | 1.42 |
| Specific gravity | 2.72 |
| Unit weight, γ [kN/m³] pri Dr = 60 % | 16.36 |
| Maximum dry unit weight [kN/m³] | 19.35 |
| Minimum dry unit weight [kN/m³] | 13.96 |
| D10 [mm] | 0.15 |
| D30 [mm] | 0.34 |
| D60 [mm] | 0.56 |
| Effective cohesion, c' [kPa] | 0.0 |
| Effective friction angle, φ' [°] | 37.00 |

### 3.3. Scale effects and applicability of model results

This study was based on a 1g small-scale physical model using dry sand; therefore, the influence of the scale effects and limitations in extrapolating the results to the prototype conditions must be acknowledged. Under 1g conditions, the initial vertical effective stress at the footing base is very low (σ'v ≈ γD ≈ 0 kPa for surface footings), and the soil response is governed by the low confining stresses, wherein the friction angle is stress-dependent and may be higher than that mobilised under field stress levels, potentially leading to an overestimation of the bearing capacity. In addition, the depth of the stress influence zone scales with the footing width (*B* = 100 mm) and may approach the tank boundaries (500 mm width) at larger spacing ratios (*x*/*B* ≥ 3), although appropriate tank dimensions and smooth side plates were adopted to minimise these boundary effects. Despite these limitations, the use of the dimensionless parameters (*x*/*B*, *e*/*B*, and *Eζ*) provides a semi-dimensional framework that enhances the interpretability and partial transferability of the results to the prototype conditions, provided that comparable soil friction angles are considered.

Similar limitations have been widely recognised in previous experimental studies on the footing interactions in sand [3, 14, 16], all of which were also conducted under 1g conditions, and reported comparable scale-related constraints. This confirms that the present study is consistent with the established experimental framework in this research area and remains comparable in scope and methodological limitations with the existing paper.

## 4. Test setup and programme

An experimental programme was designed to investigate the behaviour of a new footing subjected to eccentric loading adjacent to an existing footing. A series of small-scale model tests was conducted to achieve this objective, in a rigid steel tank under controlled laboratory conditions.

The settlements and failure mechanisms were carefully monitored to evaluate the influence of the load eccentricity and the interaction between adjacent footings. The testing procedure involved preparing a homogeneous sand bed, installing rigid model footings, and applying incremental loads by using a specially designed loading system. The existing footing was subjected to a vertical load equal to *m* × *Pu*, where *Pu* represents the ultimate bearing capacity of an isolated footing with identical geometry and soil conditions, and *m* is a load-scaling factor ranging from 0 to 1. Previous studies have typically employed *m* values of 0.33 or 0.67, corresponding to working loads with safety

**Table 2. Test programme and parameters**

| Test N° | *x*/*B* | | | | | | | *e*/*B* | | | |
|---|---|---|---|---|---|---|---|---|---|---|---|
| 1 | Isolated footing | | | | | | | 0 | | | |
| 2-3-4-5-6-7-8 | 0.5 | 1.0 | 1.5 | 2.0 | 3.0 | 4.0 | 5.0 | 0 | | | |
| 9-10-11-12 | 0.5 | | | | | | | -0.2 | -0.15 | -0.1 | -0.05 |
| 13-14-15-16 | 1 | | | | | | | -0.2 | -0.15 | -0.1 | -0.05 |
| 17-18-19-20 | 1.5 | | | | | | | -0.2 | -0.15 | -0.1 | -0.05 |
| 21-22-23-24 | 2 | | | | | | | -0.2 | -0.15 | -0.1 | -0.05 |
| 25-26-27-28 | 3 | | | | | | | -0.2 | -0.15 | -0.1 | -0.05 |
| 29-30-31-32 | 4 | | | | | | | -0.2 | -0.15 | -0.1 | -0.05 |
| 33-34-35-36 | 5 | | | | | | | -0.2 | -0.15 | -0.1 | -0.05 |
| 37-38-39-40 | 0.5 | | | | | | | 0.05 | 0.1 | 0.15 | 0.2 |
| 41-42-43-44 | 1 | | | | | | | 0.05 | 0.1 | 0.15 | 0.2 |
| 45-46-47-48 | 15 | | | | | | | 0.05 | 0.1 | 0.15 | 0.2 |
| 49-50-51-52 | 2 | | | | | | | 0.05 | 0.1 | 0.15 | 0.2 |
| 53-54-55-56 | 3 | | | | | | | 0.05 | 0.1 | 0.15 | 0.2 |
| 57-58-59-60 | 4 | | | | | | | 0.05 | 0.1 | 0.15 | 0.2 |
| 61-62-63-64 | 5 | | | | | | | 0.05 | 0.1 | 0.15 | 0.2 |

factors of approximately 3.0 and 1.5, respectively [20–22]. In this investigation, *m* was set to 0.5 to facilitate a direct comparison with the experimental results of Schmüdderich and Lavasan [22], representing an intermediate loading condition. The distance between the two footings (*x*) and the load eccentricity (*e*) were expressed in a dimensionless form to facilitate comparing the results across different footing sizes. This was done by dividing both values by the footing width (*B*), yielding the ratios *x*/*B* and *e*/*B*. Using these normalised parameters makes the results more universal and applicable to various footing configurations. The test programme is presented in Table 2.

## 5. Results and discussion

The load–settlement curves obtained from the model tests are presented to interpret the experimental findings. The analysis emphasises the effect of the existing loaded footing on the load–settlement response and ultimate bearing capacity of the new footing, considering the influence of the spacing (*x*) between the footings and the load eccentricity relative to the position of the existing footing.

In this study, the ultimate bearing capacity was determined using the tangent intersection method, which has been extensively validated through experimental studies, and is particularly valuable for granular soils. This method is well suited for soils in which the load-settlement behaviour gradually transitions from an elastic to a plastic response without a well-defined peak load [28]. This method has gained widespread acceptance in geotechnical practice because of its reliability and ease of application, making it a standard procedure recommended by various international codes and guidelines for foundation design [29]. The tangent intersection method involves constructing two tangent lines, of which the first one is drawn through the initial linear portion of the load-settlement curve, and represents the elastic response of the soil-foundation system.

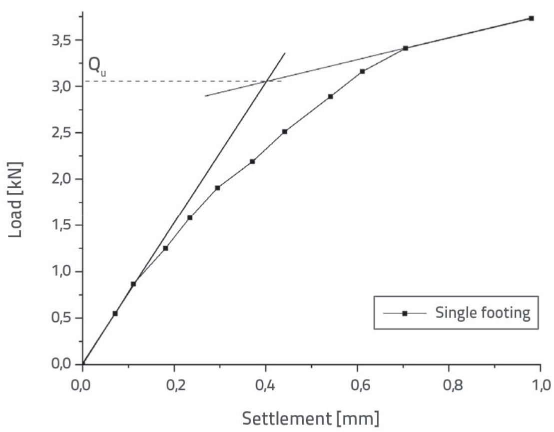


**Figure 6. Tangent intersection method for determining the ultimate load (*Qu*)**

The second tangent is drawn through the steepest portion of the nonlinear segment wherein the plastic deformation becomes dominant [28]. The point of intersection of these two tangents defines the ultimate bearing capacity, and provides a consistent and objective criterion for determining the capacity (Figure 6).

### 5.1. Load settlement curves

The load–settlement responses obtained from the 64 model tests were analysed to assess the footing behaviour under incremental loading. Figure 7 illustrates the results for the new footing subjected to centric loading at different normalised clear spacings (*x*/*B*) compared with those of the existing footing. The results demonstrated that the ultimate bearing capacity increased as *x*/*B* decreased, indicating that the proximity of the existing footing enhanced the bearing capacity of the new footing through the beneficial interaction effects. The failure load reached a maximum value of 5.44 kN at *x*/*B* = 0.5. The load–settlement curves for *x*/*B* = 3 and 4 are nearly identical to those of an isolated strip footing, indicating that the influence of the existing footing on the new footing becomes negligible at these distances. Further, the new foundation behaved as an isolated footing at these distances. Our findings agreed excellently with those of Schmüdderich and Lavasan [22] and Boufarh and Abbeche [3], who have also shown that the failure load decreases as the distance between the two footings increases.

In all the model tests, for each *x*/*B*, the new footing was loaded at varying eccentricities (*e*/*B* = 0, 0.05, 0.1, 0.15, and 0.2), as shown in Figure 8.

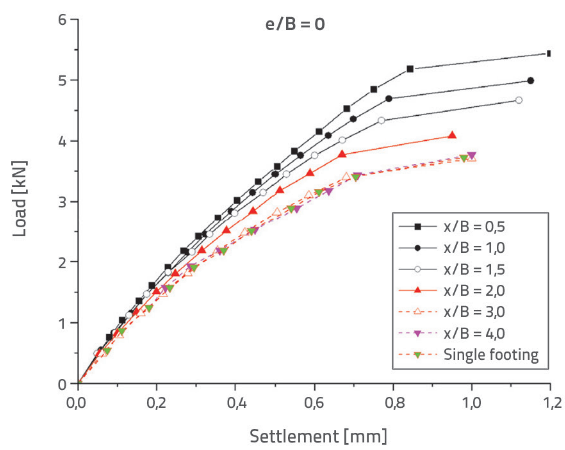


**Figure 7. Load–settlement curves of the new footing under central loading at various clear spacing ratios (*x*/*B*)**

In the present study, the existing footing was loaded before the new footing, resulting in precompression of the surrounding soil mass. For small *x*/*B* values, the stress bulb beneath the new footing significantly overlapped with the prestressed zone created by the existing footing. This overlap increased the soil confinement and stiffness, leading to smaller settlements under the same applied load, as shown in Figure 7. As the spacing ratio increased, the overlap between the stress zones decreased gradually, reducing the beneficial effects of the pre-compressed soil. Consequently, the behaviour of the new footing progressively approached that of an isolated footing, leading to larger settlements [3, 21].

Figure 8 indicates that the ultimate bearing capacity of the new footing decreases with increasing load eccentricity, which is consistent with the established principles of foundation engineering [6, 25]. Further, the ultimate bearing capacity decreased as the spacing ratio increased for both the centric and eccentric loading conditions. Specifically, the failure load reached its maximum value of 5.44 kN at *x*/*B* = 0.5, decreased to 4.69 kN at *x*/*B* = 1, and reached a minimum value of 3.71 kN at *x*/*B* = 3

For the eccentric loading cases, the results show that the ultimate bearing capacity corresponding to the positive eccentricity exceeded that corresponding to the negative eccentricity. Figure 8.a (*x*/*B* = 0.5) demonstrates that the failure load under eccentric loading reached 5.15 kN for *e*/*B* = +0.05 compared with 5.02 kN for *e*/*B* = –0.05; 4.82 kN for *e*/*B* = +0.1 and 4.35 kN for *e*/*B* = –0.1; 4.08 kN for *e*/*B* = +0.15 and 3.86 kN for *e*/*B* = –0.15; and 3.26 kN for *e*/*B* = +0.2 compared with 2.88 kN for *e*/*B* = –0.2.

Figure 8.b (*x*/*B* = 1) confirms that the ultimate bearing capacity continues to decrease as the spacing ratio increases. The directional effect of the eccentricity remains evident, with higher failure loads observed when the eccentricity is directed towards the existing footing for *e*/*B* = 0.05, 0.1, and 0.15. However, the load–settlement curves corresponding to *e*/*B* = +0.2 and *e*/*B* = –0.2 are nearly identical, indicating that the influence of the existing footing is practically eliminated for *x*/*B* > 1 and *e*/*B* > 0.2.

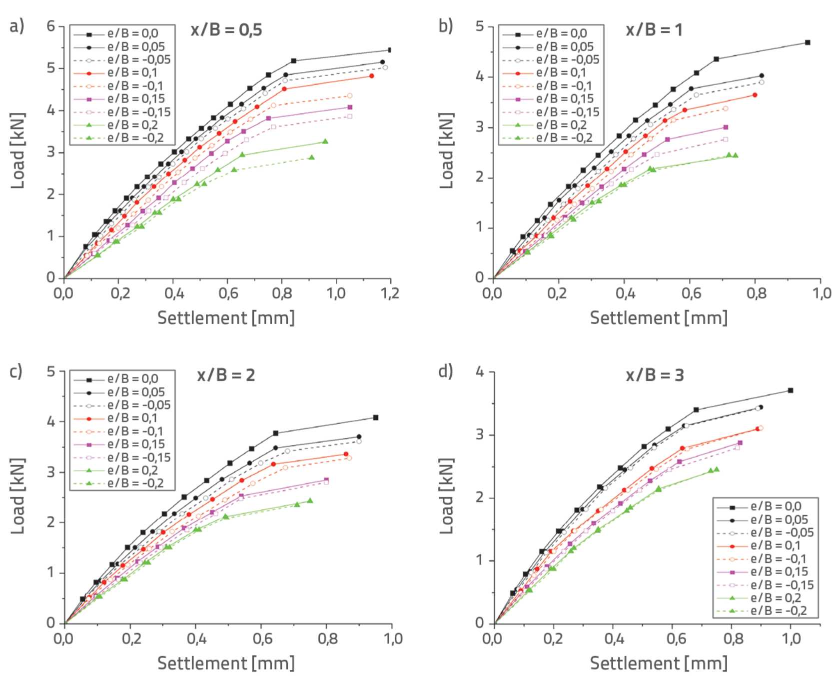


**Figure 8. Load–settlement curves of the new footing under eccentric loading at different clear spacing ratios (*x*/*B*): a) *x*/*B* = 0.5; b) *x*/*B* = 1; c) *x*/*B* = 2; d) *x*/*B* = 3**

Figure 8.c (*x*/*B* = 2) shows that the ultimate bearing capacity continues to decrease with increasing eccentricity magnitude. The difference between positive and negative eccentricities remains discernible for *e*/*B* = 0.05 and 0.1 but becomes less pronounced at higher eccentricities. The curves corresponding to *e*/*B* = ±0.15 and *e*/*B* = ±0.2 are nearly identical, suggesting that the influence of the existing footing is significantly diminished at this spacing ratio.

Finally, Figure 8.d (*x*/*B* = 3) demonstrates that the load–settlement curves for positive and negative eccentricities are essentially identical across all *e*/*B* values. This confirms that the effect of the existing footing on the new footing becomes negligible at larger spacings, and the new footing behaves as an isolated foundation.

## 5.2. Effect of the spacing ratio *x*/*B*

The parameter *x*/*B*, defined as the clear spacing between the two footings normalised by the footing width, governs the level of interaction between the foundations. An interaction factor () is introduced and defined by Eq. (1) to quantify this interaction. This factor represents the ratio of the ultimate bearing capacity of a new centrally loaded footing adjacent to an existing centrally loaded footing to that of a single isolated centrally loaded footing

$$\zeta = \frac{Q_u \text{ (centrally loaded new footing with existing centrally loaded footing)}}{Q_u \text{ (single centrally loaded footing)}} \quad (1)$$

Figure 9 presents the relationship between the interaction factor (ζ) and the clear spacing ratio (*x*/*B*) under centric loading, compared with the results reported by Kouzer and Kumar [20]. The results demonstrate that the interaction factor decreases as *x*/*B* increases. For *x*/*B* > 3, ζ becomes nearly constant and approaches 1, indicating that the ultimate bearing capacity of the new footing adjacent to an existing footing is identical to that of an isolated footing. In this case, the influence of the existing footing is eliminated when x/B > 3.

Comparing the present experimental results with those of Kouzer and Kumar [20] showed reasonable agreement. However, the values reported by Kouzer and Kumar [20] were slightly higher than those obtained in this study for small clear spacing ratios (e.g. *x*/*B* = 0.5). This discrepancy can be attributed to the fact that numerical studies generally yield higher values than experimental investigations, owing to the idealised boundary conditions and absence of experimental uncertainties.

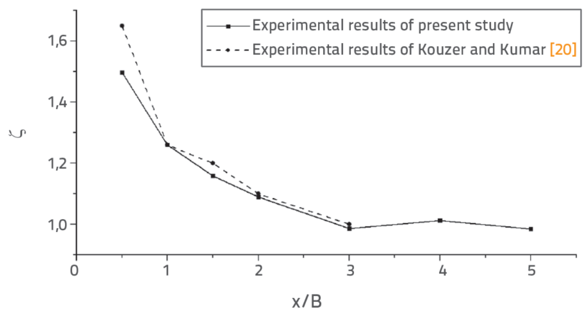


**Figure 9. Variation of the interaction factor (ζ) with respect to *x/B* under centric loading**

In the present study, a new eccentric interaction factor (Eζ) is introduced, as defined by Eq. (2). This eccentric interaction factor represents the ratio of the ultimate bearing capacity of a new eccentrically loaded footing adjacent to an existing centrally loaded footing to that of a single isolated centrally loaded footing.

$$E\zeta = \frac{Q_u\,(\text{eccentric new footing with existing centrally loaded footing})}{Q_u\,(\text{single centrally loaded footing})} \qquad (2)$$

Figure 10 demonstrates that the *Eζ* of the new strip footing decreases as *x/B* increases, regardless of whether the eccentricity is positive or negative. *Eζ* exceeds 1 for small eccentricity ratios (i.e., *e/B* ≤ 0.1) (Figure 10(a)), reaching maximum values of 1.40 for *e/B* = +0.05, 1.30 for *e/B* = −0.05, 1.18 for *e/B* = +0.10, and 1.05 for *e/B* = −0.10 at *x/B* = 0.5. This indicates that for *x/B* < 0.5, the ultimate bearing capacity of an eccentrically loaded strip footing adjacent to an existing footing of identical width exceeds that of an isolated footing under centric loading, particularly for small eccentricity ratios (i.e., *e/B* ≤ 0.1). The results also reveal that the ultimate bearing capacity was greater when the eccentricity was directed towards the existing footing than when the eccentricity was directed away from it. Moreover, *Eζ* becomes nearly identical for the positive and negative eccentricities at *x/B* > 3, indicating that the behaviour of the new footing becomes independent of the existing footing at larger spacing ratios , especially for small eccentricity ratios (i.e., *e/B* ≤ 0.1). Figure 10(b) indicates that *Eζ* follows the same decreasing trend with increasing spacing ratio for eccentricity ratios between 0.15 and 0.2, regardless of the eccentricity direction. However, *Eζ* < 1 and becomes nearly identical for *x/B* ≥ 1.5. This indicates that the influence of the existing footing becomes negligible, and the footing under eccentric loading with 0.15 ≤ *e/B* ≤ 0.2 behaves essentially as an isolated footing. The effect of the eccentricity direction (towards or away from the existing footing) is noticeable for *x/B* ≤ 1.5 at *e/B* = 0.15 and for *x/B* ≤ 1 at *e/B* = 0.2.

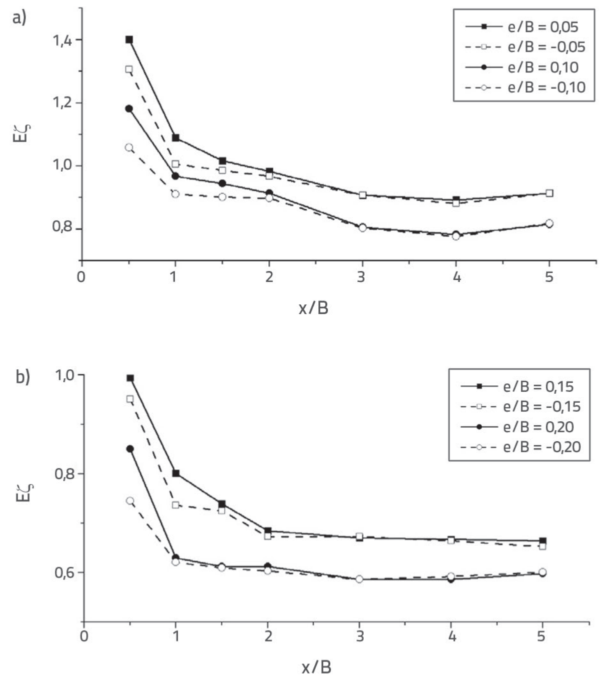


**Figure 10. Variation of the eccentric interaction factor (Eζ) with x/B**

### 5.3. Failure mechanism

In the case of a new footing placed near an existing footing, when the spacing between them was small, the primary failure surface extended beneath the existing footing, and the shear interaction between the footings was significant. However, as the spacing increased, for example, at *x/B* = 3, the failure mechanism transitioned to a nearly symmetrical shape, similar to that of an isolated footing [22]. Under eccentric loading,the failure surfaces become asymmetric, owing to the footing tending to tilt towards the side of the eccentricity, resulting in the development of a primary failure surface on the eccentric side and a secondary failure surface on the opposite side[5, 6, 8, 9, 26].

In the present study, for a small spacing ratio (*x/B* = 0.5, Figure 11), when the eccentric load was applied towards the existing footing (Figure 11(a): *e/B* = + 0.1), the primary failure zone extended beneath the existing footing, while the secondary failure zone formed on the opposite side (mechanism Type A+). Conversely, for *e/B* = −0.1 (Figure 11(b)), the primary failure zone shifted to the side farther from the existing footing, whereas the secondary zone developed beneath it (mechanism Type A-).

These findings demonstrate that the direction of the load eccentricity is decisive in shaping the load transfer and the evolution of the failure mechanisms: positive eccentricities

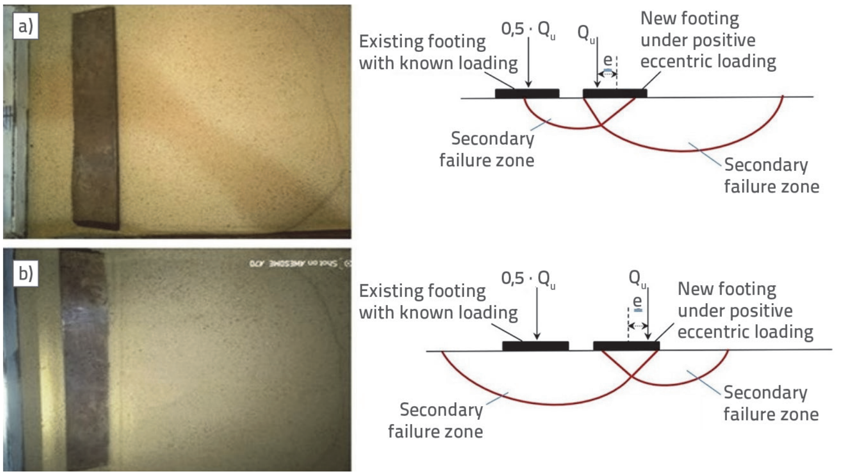


**Figure 11. Failure mechanism of the soil beneath a strip footing under eccentric loading for a relative spacing of *x*/*B* = 0.5: a) Mechanism Type A+ (*e*/*B* = 0.1); b) Mechanism Type A- (*e*/*B* = –0.1)**

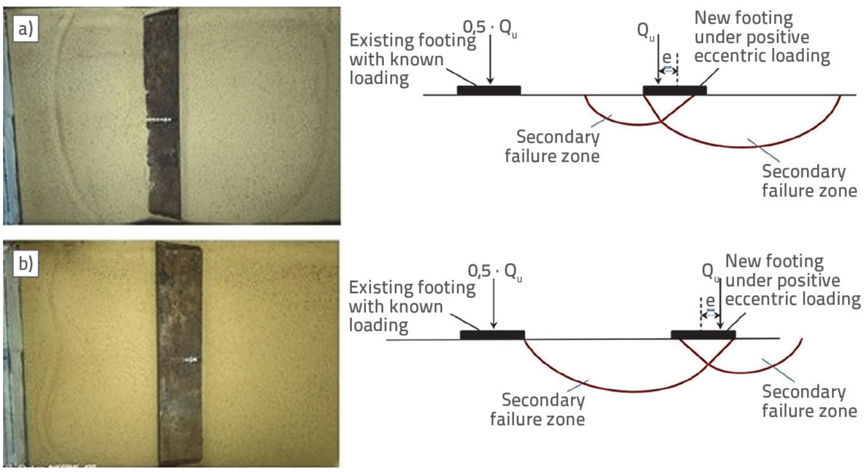


**Figure 12. Failure mechanism of the soil beneath a strip footing under eccentric loading for a relative spacing of *x*/*B* = 3: a) Mechanism Type B+ (*e*/*B* = +0.1); b) Mechanism Type B- (*e*/*B* = –0.1)**

(A+) enhance the interaction with the existing footing and lead to higher eccentric interaction factors, whereas negative eccentricities (A-) tend to reduce this interaction.

For a larger spacing ratio (*x*/*B* = 3, Figure 12), the observed failure mechanism evolved from Type A to Type B, with B+ corresponding to the positive eccentricity (load applied towards the existing footing) and B- to the negative eccentricity (load applied away from the existing footing). With this increased spacing, the primary failure zone no longer propagated beneath the existing footing. Instead, it was predominantly confined beneath the newly constructed footing, extending only to the vicinity of the existing footing, and the overlap between the two zones was negligible. This change in the failure mechanism indicated that the direct structural interaction between the two footings was largely eliminated at this spacing. The secondary failure zone, which was significant at lower spacing ratios (*x*/*B* = 0.5), became significantly smaller and did not penetrate beneath the existing footing at *x*/*B* = 3. This reflected a substantial reduction in the interference effects, indicating that the stress transfer and load redistribution between the two footings were minimal. Consequently, the interaction factor approached 1, indicating that the ultimate bearing capacity and settlement response of the new footing were nearly identical to those of the footing constructed without any existing foundation nearby.

Under these conditions, the load transfer mechanism closely resembled that of an independent (isolated) footing, with negligible influence from the preexisting footing. In conclusion, increasing the spacing ratio from *x*/*B* = 0.5 to *x*/*B* = 3 results in a clear evolution of the failure mechanism: at small spacing, the mechanism is dominated by Type A+ when the eccentric load is directed towards the existing footing and Type A- when it is directed away; as the spacing increases to *x*/*B* = 3, these mechanisms transition to Type B+ and B-, where the interference effect becomes minimal, and the new footing behaves nearly as an isolated foundation.

## 6. Conclusions

The behaviour of eccentrically loaded strip footings placed near existing footings was experimentally investigated through 64 model tests, focusing on the effects of the spacing ratio (*x*/*B*) and load eccentricity (*e*/*B*). Based on the results, the following conclusions were drawn:

- The bearing capacity of a new footing is significantly influenced by an adjacent footing at small spacing ratios *x*/*B* ≤ 1, particularly when the load eccentricity is directed towards the existing footing. Under these conditions, the interaction effects enhanced the load capacity with a maximum value of 5.44 kN recorded at *x*/*B* = 0.5.
- The interaction effect decreases with increasing spacing and becomes negligible for *x*/*B* ≥ 3, wherein the new footing behaves as an isolated foundation.

- The eccentric interaction factor decreases with increasing spacing and approaches 1 at large separations. At small eccentricities $e/B \leq 0.1$ and close spacing $x/B = 0.5$, exceeds 1, reaching values of 1.40 and 1.30 for the positive and negative eccentricities, respectively.
- Two failure mechanisms were identified: an interaction-dominated mechanism at small spacing $x/B \leq 1$, and an independent mechanism at larger spacing $x/B \geq 3$.
- The load eccentricity direction significantly affected the performance, with the eccentricity towards the existing footing resulting in a higher bearing capacity compared with the opposite direction.
- These results highlight the necessity of considering the footing interactions and load eccentricity when designing closely spaced foundations.
- Although the present study provides valuable experimental insights into the interference behaviour between footings, certain limitations should be acknowledged. This investigation was limited to experimental observations without complementary numerical verification. Although the results capture the overall load–settlement response reliably, numerical modelling would enable assessing the underlying stress–strain mechanisms in more detail.
- Therefore, future research should incorporate advanced numerical approaches, such as finite element or finite difference methods (e.g., PLAXIS 3D), to reproduce and validate the experimental findings. Such analyses would facilitate a comprehensive visualisation of the stress and strain distributions within the soil and provide further insights into the interaction mechanisms. In addition, extended parametric studies are recommended to evaluate the influence of the embedment depth, a wider range of soil densities, and varying load levels applied to the existing footing. These aspects represent key directions for the further development of the present study.

## REFERENCES


[1] Chandrawanshi, S., Garg, V.: Effect of adjacent structures on footing settlement for different multi-building arrangements, Open Engineering, 14 (2024) 1, https://doi.org/10.1515/eng-2024-0092.

[2] Das, B.M., Larbi-Cherif, S.: Bearing Capacity of Two Closely-Spaced Shallow Foundations on Sand, Soils and Foundations, 23 (1983) 1, pp. 1–7, https://doi.org/10.3208/sandf1972.23.1.

[3] Boufarh, R., Abbeche, K., Abdi, A.: Experimental Investigation of Interference Between Adjacent Footings on Layered Cohesionless Soil, Soil Mechanics and Foundation Engineering, 56 (2019), pp. 128–135, https://doi.org/10.1007/s11204-019-09580-z.

[4] Folić, R., Bonić, Z.: Punching of column footings – comparison of experimental and calculation results, GRAĐEVINAR, 65 (2013) 10, pp. 887–899, https://doi.org/10.14256/JCE.916.2013.

[5] Terzaghi, K.: Theoretical Soil Mechanics, John Wiley & Sons, New York, 1943, https://doi.org/10.1002/9780470172766.

[6] Meyerhof, G.G.: Some Recent Research on the Bearing Capacity of Foundations, Canadian Geotechnical Journal, 1 (1963), pp. 16–26, https://doi.org/10.1139/T63-003.

[7] De Beer, E.E.: Experimental Determination of the Shape Factors and the Bearing Capacity Factors of Sand, Géotechnique, 20 (1970) 4, pp. 387–411, https://doi.org/10.1680/geot.1970.20.4.387.

[8] Prakash, S., Saran, S.: Bearing Capacity of Eccentrically Loaded Footings, Journal of the Soil Mechanics and Foundations Division (ASCE), 97 (1971), pp. 95–117, https://doi.org/10.1061/JSFEAQ.0001544.

[9] Sadoglu, E., Cure, E., Moroglu, B., Uzuner, B.A.: Ultimate Loads for Eccentrically Loaded Model Shallow Strip Footings on Geotextile-Reinforced Sand, Geotextiles and Geomembranes, 27 (2009), pp. 176–182, https://doi.org/10.1016/j.geotexmem.2008.11.002.

[10] Das, S., Maheshwari, B.K.: Bearing Capacity of Strip Footings on Slopes Under Eccentric and Inclined Loads, Geotechnical and Geological Engineering, 2025, https://doi.org/10.1007/s10706-024-03053-3.

[11] Stuart, J.G.: Interference Between Foundations, with Special Reference to Surface Footings in Sand, Géotechnique, 12 (1962) 1, pp. 15–22, https://doi.org/10.1680/geot.1962.12.1.15.

[12] Trask, P.D.: Soil Mechanics in Engineering Practice by Karl Terzaghi and Ralph B. Peck, The Journal of Geology, 57 (1949), pp. 622–623, https://doi.org/10.1086/625679.

[13] Nainegali, L., Ekbote, A. G.: Interference of Two Nearby Footings Resting on Clay Medium, Lecture Notes in Civil Engineering, Springer, Singapore, 2018, pp. 59–67, https://doi.org/10.1007/978-981-13-0368-5_7.

[14] Kumar, J., Bhoi, M.K.: Interference of Two Closely Spaced Strip Footings on Sand Using Model Tests, Journal of Geotechnical and Geoenvironmental Engineering, 135 (2009) 4, pp. 595–604, https://doi.org/10.1061/(ASCE)1090-0241(2009)135:4(595).

[15] Mabrouki, A., Benmeddour, D., Frank, R., Mellas, M.: Numerical Study of the Bearing Capacity for Two Interfering Strip Footings on Sands, Computers and Geotechnics, 37 (2010), pp. 431–439, https://doi.org/10.1016/j.compgeo.2009.12.007.

[16] Gupta, A., Sitharam, T.G.: Experimental and Numerical Investigations on Interference of Closely Spaced Square Footings on Sand, International Journal of Geotechnical Engineering, 14 (2018), pp. 142–150, https://doi.org/10.1080/19386362.2018.1454386.

[17] Ghosh, P., Kumar, S.: Interference Effect of Two Nearby Strip Surface Footings on Cohesionless Layered Soil, International Journal of Geotechnical Engineering, 5 (2011), pp. 87–94, https://doi.org/10.3328/IJGE.2011.05.01.87-94.

[18] Ghazavi, M., Fazeli Dehkordi, P.: Interference Influence on Behavior of Shallow Footings Constructed on Soils, Past Studies to Future Forecast: A State-of-the-Art Review, Transportation Geotechnics, 27 (2021), Article 100502, https://doi.org/10.1016/j.trgeo.2020.100502.

[19] Ekbote, A.G., Nainegali, L.: Interference of Two Closely Spaced Strip Footings Embedded in Cohesionless Fibre-Reinforced Foundation Soil Bed, Geo-Congress 2019, American Society of Civil Engineers, Reston, 2019, pp. 454–464, https://doi.org/10.1061/9780784482094.041.

[20] Kouzer, K.M., Kumar, J.: Ultimate Bearing Capacity of a Footing Considering the Interference of an Existing Footing on Sand, Geotechnical and Geological Engineering, 28 (2010), pp. 457–470, https://doi.org/10.1007/s10706-010-9305-9.

[21] Nainegali, L., Basudhar, P.K., Ghosh, P.: Interference of Proposed Footing with an Existing Footing Resting on Non-Linearly Elastic Dense and Loose Cohesionless Soil Bed, European Journal of Environmental and Civil Engineering, 25 (2021), pp. 2574–2591, https://doi.org/10.1080/19648189.2019.1638311.

[22] Schmüdderich, C., Lavasan, A.A., Tschuchnigg, F., Wichtmann, T.: Bearing Capacity of a Strip Footing Placed Next to an Existing Footing on Frictional Soil, Soils and Foundations, 60 (2020), pp. 229–238, https://doi.org/10.1016/j.sandf.2020.03.002.

[23] British Standards Institution: Eurocode 7: Geotechnical Design – Geotechnical Structures, BSI, London, https://doi.org/10.3403/30402003U.

[24] Frank, R., Bauduin, C., Driscoll, R., Kavvadas, M., Krebs Ovesen, N., Orr, T., Schuppener, B.: Designers' Guide to EN 1997-1 Eurocode 7: Geotechnical Design – General Rules, Thomas Telford Publishing, London, 2005, https://doi.org/10.1680/dgte7.31548.

[25] Pantelidis, L., Meddah, A.: The Effect of Loading Inclination and Eccentricity on the Bearing Capacity of Shallow Foundations: A Review, Archives of Computational Methods in Engineering, 31 (2024), pp. 4189–4208, https://doi.org/10.1007/s11831-024-10113-7.

[26] Kaya, N., Örnek, M., Türedi, Y.: Ultimate Loads for Eccentrically Loaded Skirted Strip Footings on Sand, Proceedings of the XVI European Conference on Soil Mechanics and Geotechnical Engineering, ICE Publishing, 2015, pp. 3413–3418, https://doi.org/10.1680/ecsmge.60678.vol6.535.

[27] ASTM International: Standard Practice for Classification of Soils for Engineering Purposes (Unified Soil Classification System), ASTM D2487-17, ASTM International, West Conshohocken, PA, 2017, https://doi.org/10.1520/D2487-17.

[28] Trautmann, C.H., Kulhawy, F.H.: Uplift Load-Displacement Behavior of Spread Foundations, Journal of Geotechnical Engineering, 114 (1988) 2, pp. 168–184, https://doi.org/10.1061/(ASCE)0733-9410(1988)114:2(168).

[29] Das, B.M.: Uplift Capacity of Shallow Foundations, u: Shallow Foundations, CRC Press, Boca Raton, 1999, pp. 465–498, https://doi.org/10.1201/9781482271305-18.